

Gibbs' Energy of Formation of Nickel Orthosilicate (Ni_2SiO_4)

K.T. Jacob*, G.M. Kale*, Akila Ramachandran[†]* and A.K. Shukla**

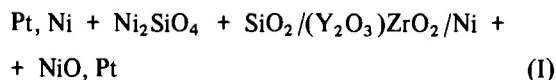
*Department of Metallurgy, [†]Materials Research Laboratory, **Solid State and Structural Chemistry Unit
Indian Institute of Science, Bangalore 560 012, India

CONTENTS

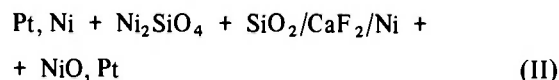
	Page
ABSTRACT	142
1. INTRODUCTION	142
2. EXPERIMENTAL PROCEDURE	143
2.1. Materials	143
2.2. Solid State Cell with $(\text{Y}_2\text{O}_3)_2\text{ZrO}_2$ Electrolyte	143
2.3. Solid State Cell with CaF_2 Electrolyte	144
3. RESULTS	144
3.1. Cell with $(\text{Y}_2\text{O}_3)_2\text{ZrO}_2$ Electrolyte	144
3.2. Cell with CaF_2 Electrolyte	145
4. DISCUSSION	146
4.1. Gibbs' Energy of Formation of Ni_2SiO_4 (olivine)	146
4.2. Gibbs' Energy of Formation of Ni_2SiO_4 (spinel)	147
4.3. Conduction Mechanism in CaF_2 with Oxygen Electrodes	147
5. SUMMARY	147
REFERENCES	148

ABSTRACT

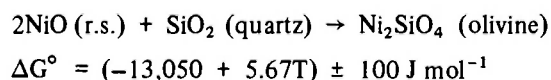
Two solid state galvanic cells:



and



have been employed for the determination of the Gibbs' energy of formation of nickel orthosilicate (Ni_2SiO_4) from nickel oxide and quartz. The emf of cell (I) was reversible and reproducible in the temperature range 925 to 1375K whereas emf of cell (II) drifted with time and changed polarity. From the results of cell (I), the Gibbs' energy of formation of nickel silicate is obtained as,



Gibbs' energy of formation of the spinel form of Ni_2SiO_4 is obtained by combining the data for olivine obtained in this study with high pressure data on olivine to spinel transition reported in the literature.

The complex time dependence of the emf of cell (II) can be rationalised on the basis of formation of calcium silicates from calcium oxide, generally present as an impurity in the calcium fluoride electrolyte, and silica. The emf of cell (II) is shown to be the function of the activity of calcium oxide at the electrolyte/electrode interface. The results provide strong evidence against the recent suggestion of mixed anionic conduction in calcium fluoride.

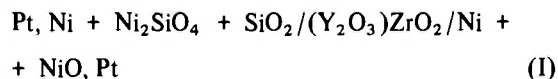
1. INTRODUCTION

Nickel orthosilicate (Ni_2SiO_4), which occurs in nature as mineral liebenbergite, has interesting high temperature properties. It decomposes to nickel oxide and silica at high temperatures, and converts from olivine to spinel at high pressures. The decomposition temperature has been reported as 1923K by Ringwood /1/ and 1818K by Phillips *et al.* /2/. Ni_2SiO_4 forms a continuous series of solid solutions with Mg_2SiO_4 . Thermodynamic data on Ni_2SiO_4 is of interest to pyrometallurgy and geochemistry.

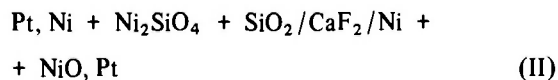
Gibbs' energy of formation of Ni_2SiO_4 (olivine) has been measured earlier by Taylor and Schmalzried

/3/ using an emf technique between 1073 and 1373K, Campbell and Roeder /4/ (1573 to 1773K), and Lebedev and Levitskii /5/ (1073 to 1373K) using CO/CO_2 equilibrium technique. Recently Rög and Rög /6/ have measured the Gibbs' energy of formation at 967 and 1170K using a nickel substituted β "-alumina solid electrolyte. Although the crystallographic form of silica used in these studies is not explicitly stated, it is reasonable to assume that the high quartz form was used by Taylor and Schmalzried /3/, Lebedev and Levitskii /5/ and Rög and Rög /6/, and high cristobalite was produced in the reduction of Ni_2SiO_4 by CO at the temperatures used by Campbell and Roeder /4/. The enthalpy of formation of Ni_2SiO_4 (olivine) from component oxides NiO (rock salt) and SiO_2 (high quartz) at 965K was measured calorimetrically by Navrotsky /7/ using molten $2\text{PbO} \cdot \text{B}_2\text{O}_3$ as the solvent. The enthalpy of formation is $(-13.9) \pm 1.9 \text{ kJ mol}^{-1}$.

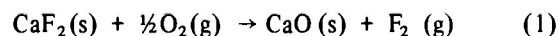
This paper reports a redetermination of the Gibbs' energy of formation of Ni_2SiO_4 (olivine) using two solid state galvanic cells:



and

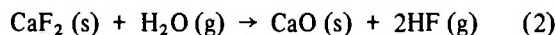


The silica used had the β -quartz structure. The $(\text{Y}_2\text{O}_3)\text{-ZrO}_2$ electrolyte is a well known oxygen ion conductor with an ionic transport number, $t_{\text{O}^{2-}}$, greater than 0.99 at oxygen partial pressures established at the electrodes in the temperature range covered in this study. The CaF_2 solid electrolyte is a fluorine ion conductor which, on being employed in combination with oxide electrodes, has been found to generate the cell potential of an oxygen concentration cell, akin to an oxygen ion conductor /8, 9, 10/. This phenomenon may be attributed to the ability of CaF_2 to transport oxygen ions in addition to fluorine ions /9/ or, following the explanation of Jacob *et al.* /11/ for analogous sulphide electrodes, to the presence of CaO particles in CaF_2 /10/. The presence of CaO converts the oxygen potential established by the oxide electrodes into an equivalent fluorine potential by virtue of the exchange reaction,



provided both CaF_2 and CaO are maintained at known

activities at both the electrodes. Thermal treatment of CaF_2 usually produces a precipitate of small particles of CaO , which can be readily observed under a scanning electron microscope and identified by selected area electron diffraction. The CaO precipitates result from the reaction of CaF_2 with traces of water vapour at high temperatures through the reaction,



It is observed that dry oxygen does not react with CaF_2 to produce CaO . The activities of CaF_2 and CaO in the solid electrolyte are unity as the mutual solubility between the two is negligible.

2. EXPERIMENTAL PROCEDURE

2.1. Materials

Puratronic grade Ni and NiO powders were obtained from Johnson Matthey Chemicals Ltd. Silica of 99.9% purity was obtained from Ventron. Nickel orthosilicate was prepared from high-purity silicic acid and nickel sulphate. Both compounds were heated separately in flowing argon up to 1400K, and their respective mass losses were determined. An intimate mixture of two compounds in the appropriate ratio was then heated to 1200K in a platinum crucible in an atmosphere of argon. After quenching, the mixture was ground under acetone, pelletized, and fired at 1750K. The cycle of quenching, grinding, pelletizing and firing at 1750K was repeated four times. The mixture was held at 1750K for a total of 5 days. X-ray diffraction analysis indicated that the product was single phase.

The three phase electrode pellets were made by mixing powders of Ni, Ni_2SiO_4 and SiO_2 (quartz) in equimolar ratio, pelletizing and sintering at 1250K. The reference electrode contained an equimolar mixture of Ni and NiO. For use in cell (II), reference electrode pellets were sintered at 1400K. The electrode pellets were polished before use in the cell.

Single crystal optical grade CaF_2 rods of 1.27 cm diameter, grown along $\langle 111 \rangle$ direction, were purchased from Harshaw Chemical Company. Discs of 0.4 cm thickness were cut from the rods using a diamond wheel. Yttria stabilized zirconia tubes, closed at one end, were obtained from Zirconium Corporation of America.

2.2. Solid State Cell with $(\text{Y}_2\text{O}_3)/\text{ZrO}_2$ Electrolyte

A schematic diagram of the apparatus incorporating

$(\text{Y}_2\text{O}_3)/\text{ZrO}_2$ tube is shown in Fig. 1. The Ni + NiO

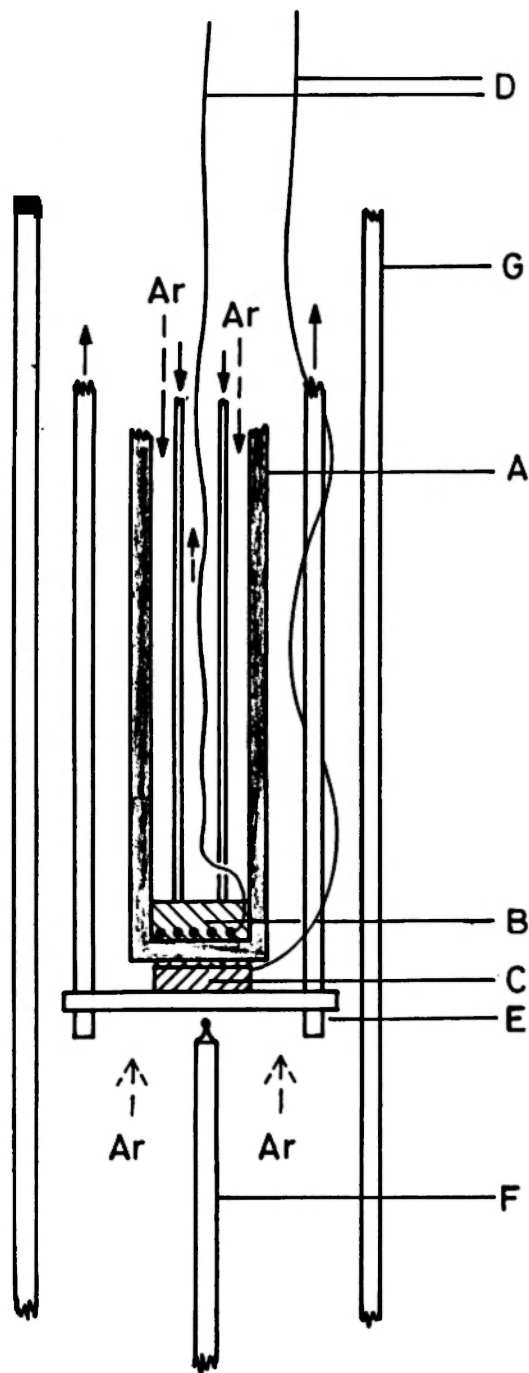


Fig. 1. Schematic diagram of the solid state galvanic cell with $(\text{Y}_2\text{O}_3)/\text{ZrO}_2$ electrolyte. A – $(\text{Y}_2\text{O}_3)/\text{ZrO}_2$ electrolyte tube; B – Ni + NiO reference electrode; C – Ni + Ni_2SiO_4 + SiO_2 electrode; D – Pt leads; E – Alumina slabs and rods for spring loading; F – Pt/Pt-13% Rh thermocouple; G – Outer alumina tube enclosing the cell inside which an inert atmosphere is maintained.

reference electrode was prepared by compacting the powder mixture against the closed end of the tube and sintering *in situ* in argon at 1400K with a platinum lead buried in the mixture. The three phase electrode was spring loaded against the outside surface of the tube by a system of alumina slabs and rods. A platinum gauze was inserted between the electrode pellet and solid electrolyte. A platinum lead was spot welded to the gauze. Each electrode was flushed by a separate purified stream of argon. Oxygen transport via the vapour phase between the two electrodes is prevented by this cell arrangement.

The emf of the cell was measured with a Princeton Applied Research (Model PAR 136) high-impedance digital voltmeter. The reversibility of the cell was checked by passing small currents (ca. $50 \mu\text{A}$) through the cell in either direction for 200 s. In each case the emf was found to return to the original value before coulometric titration. The emf was also independent of the flow rate of argon through the cell in the range of 1 to 4 ml s^{-1} . The emfs were reproducible on repeated temperature cycling.

The temperature of the cell was measured by a Pt/Pt-13%Rh thermocouple placed adjacent to the three phase electrode. To check for the absence of thermal gradient, the emf of a symmetric cell with Ni + NiO electrodes on both sides of the solid electrolyte was measured from 900 to 1400K. The emf was less than $\pm 0.2 \text{ mV}$ at all temperatures without any systematic trends. At the end of the experiments, the electrodes were examined by X-ray diffraction. The phase composition of the electrodes was found to be unaltered during the experiment.

After a change of temperature, the emf of the cell attained equilibrium values in 4 to 12 ks. The slow response is probably related to the kinetics of the reaction between the three condensed phases.

2.3. Solid State Cell with CaF_2 Electrolyte

A schematic diagram of the stacked pellet assembly with single crystal CaF_2 solid electrolyte is shown in Fig. 2. A single stream of argon flows over both the electrodes. Use of this simple configuration was dictated by the nonavailability of long CaF_2 tubes. The emf of this cell changed with time as described in section 3.2. All other experimental details were similar to those given in section 2.2.

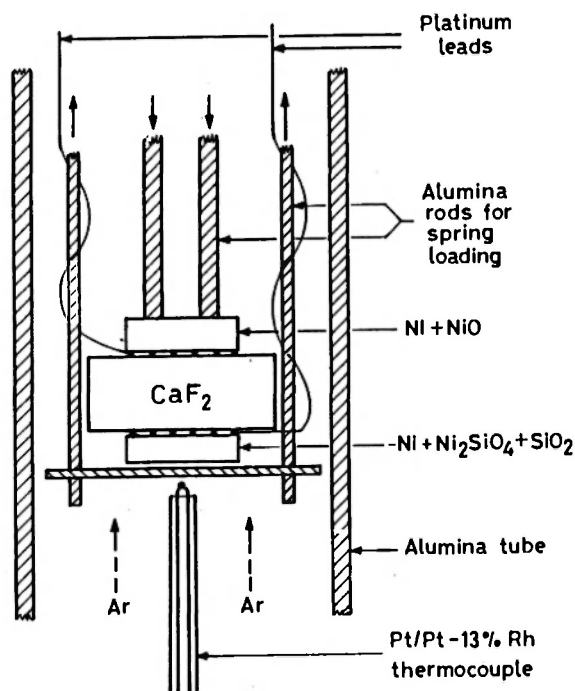


Fig. 2. Cell arrangement with CaF_2 single crystal solid electrolyte (cell II).

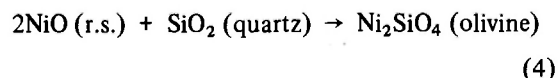
3. RESULTS

3.1. Cell with $(\text{Y}_2\text{O}_3)_3\text{ZrO}_2$ Electrolyte

The reversible emf of cell (I) is plotted as a function of temperature in Fig. 3. The numbers shown on the figure indicate the sequence of measurement. The least-mean-squares regression analysis gives

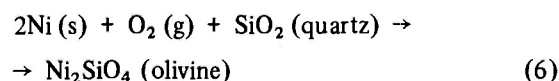
$$E = (33.82 - 1.47 \times 10^{-2} T) \pm 0.4 \text{ mV} \quad (3)$$

The emf is directly related to the Gibbs' energy of formation of Ni_2SiO_4 (olivine) from nickel oxide (rock salt) and silica (high quartz). For the reaction,



$$\Delta G^\circ = (-13,050 + 5.67T) \pm 100 \text{ J mol}^{-1} \quad (5)$$

By combining the above equation with the standard free energy of formation of nickel oxide [12] one obtains for the reaction,



$$\Delta G^\circ = (-481,140 + 175.5T) \pm 1000 \text{ J mol}^{-1} \quad (7)$$

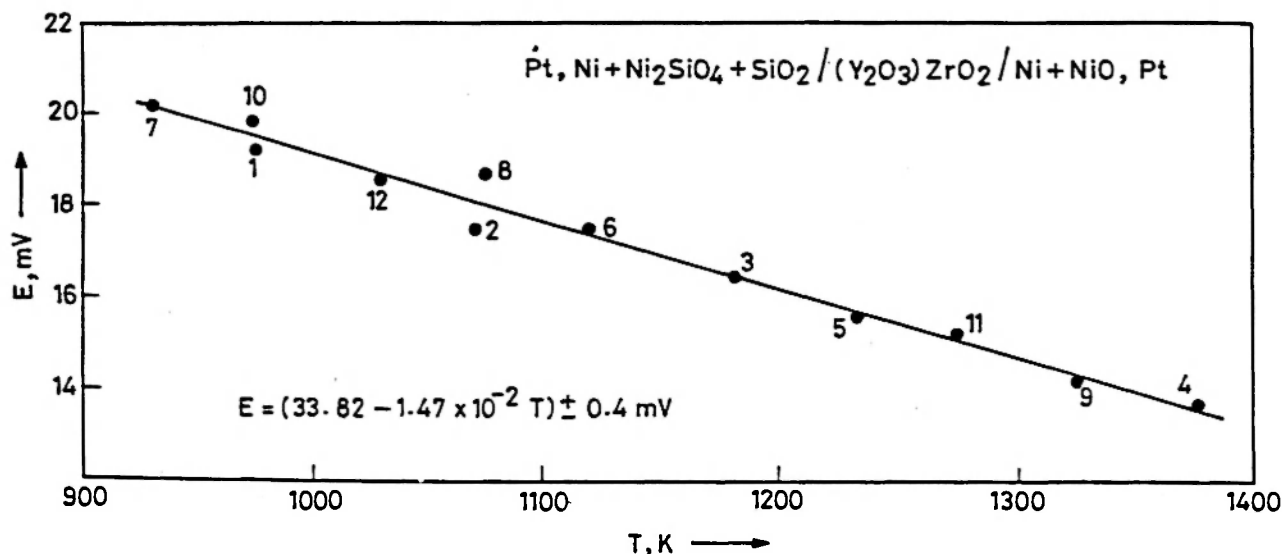


Fig. 3. Temperature dependence of the emf of cell (I) with $(Y_2O_3)ZrO_2$ solid electrolyte.

3.2. Cell with CaF_2 Electrolyte

At the beginning of the experiment the emf of cell (II) was approximately ± 2.5 mV, the same as that obtained with cell (I). However, the emf gradually decreased with time and changed polarity. The change in emf with time is plotted in Fig. 4 at 975K; identical patterns were obtained by starting the experiment at higher temperatures. The zero point on the time axis is arbitrarily set when the emf reaches its maximum value close to that of cell (I). Three plateau regions corresponding to -43 mV, -402 mV and -441 mV are seen on the emf plot. The emf was stable at -441 (± 2) mV for up to 20 ks. This emf was partially reversible (± 5 mV) when small currents (ca. $50 \mu A$) were passed in either direction. On increasing the temperature to 1300K, the emf remained virtually unaltered (± 5 mV). At the end of the experiments, the CaF_2 electrolyte had a milky appearance, with an apparently greater volume fraction of precipitate particles at the surface in contact with the three phase electrode. Selected area electron diffraction has revealed the presence of $CaSiO_3$ at this surface.

The rather unexpected response of cell (II) can be rationalized by considering the interaction between CaO at the surface of the solid electrolyte and free silica in the electrode pellet. Phase diagram for the $CaO-SiO_2$ system [13] shows three stable silicates at 975K viz., Ca_2SiO_4 , $Ca_3Si_2O_7$ and $CaSiO_3$. At the beginning of the experiment, if pure CaO is present on both surfaces of the solid electrolyte, the emf should

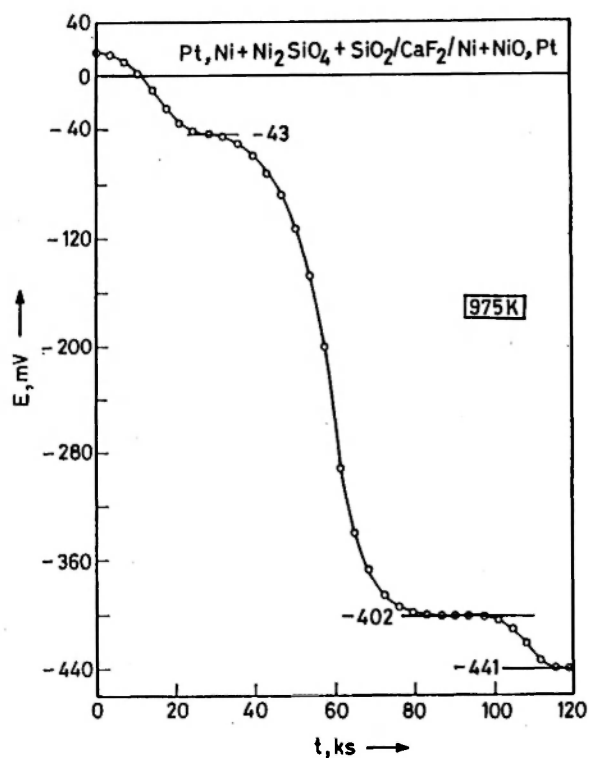


Fig. 4. Variation of the emf of cell (II) incorporating CaF_2 electrolyte with time at 975K.

be the same as for cell (I). At each electrode the oxygen potential is converted to an equivalent fluorine potential by virtue of exchange reaction (1). The phase diagram for the $NiO-CaO$ system [13] shows only small solid

solubility (less than 1 mol pct), without compound formation. Hence no significant reaction is expected between NiO and CaO at the electrolyte/electrode interface. However, with the passage of time CaO can react with SiO_2 in the three phase electrode to produce the stable silicate phases. The calcium oxide activity will progressively decrease from unity as higher silicates are formed. Benz and Wagner /14/ have measured the activity of CaO as a function of SiO_2 concentration in the CaO- SiO_2 system at 973K. The activity remains constant in the two phase fields. The calculated decrease in emf due to the presence of different silicates at the electrode/electrolyte interface is summarized in Table 1. The plateau emfs closely match (± 2 mV) the sum of the initial emf and the expected decrease due to silicate formation.

TABLE 1: Chemical potential of CaO /12/ and change in emf of cell (II) for different phase mixtures of CaO- SiO_2 system at the electrode/electrolyte interface at 973K

Phase Mixture	$\Delta\mu_{\text{CaO}}$, kJ /14/	ΔE , mV
CaO + Ca_2SiO_4	0	0
Ca_2SiO_4 + $\text{Ca}_3\text{Si}_2\text{O}_7$	-11.72	-60.7
$\text{Ca}_3\text{Si}_2\text{O}_7$ + CaSiO_3	-80.75	-418.4
CaSiO_3 + SiO_2	-89.12	-461.8

4. DISCUSSION

4.1. Gibbs' Energy of Formation of Ni_2SiO_4 (olivine)

The standard free energy of formation of Ni_2SiO_4 obtained in this study is compared in Fig. 5 with earlier measurements reported in the literature wherein the form of silica participating in the reaction is not explicitly given. The value obtained in this study with NiO (rock salt) and SiO_2 (β -quartz) as standard states agrees with the result of Taylor and Schmalzried /3/ at 1020K, but the slopes of the curves differ significantly. The difference can be partially narrowed if SiO_2 used by Taylor and Schmalzried /3/ was β -tridymite or β -cristobalite. The results of Rög and Rög /6/ closely parallel those of reference /3/. The free energy corresponding to reaction (4) given by Lebedev and Levitskii /5/ are more negative by 13.70 kJ at 1073 and 16.86 kJ at 1373K than those obtained in this study and fall outside the range of Fig. 5. During the decomposition studies by Campbell and Roeder

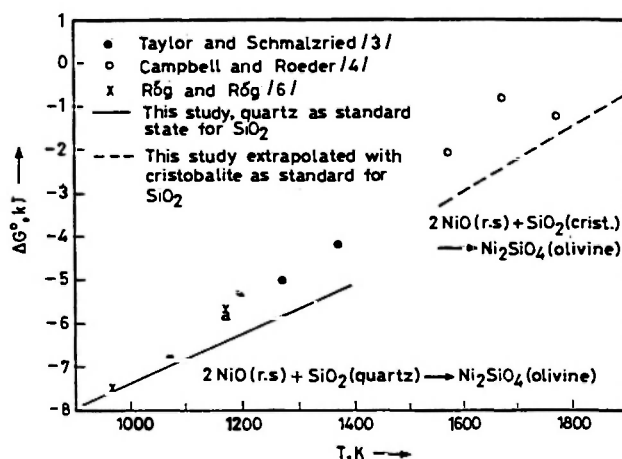


Fig. 5. Comparison of the Gibbs' energy of formation of Ni_2SiO_4 (olivine) from component oxides obtained in this study with data reported in the literature.

/4/ under $\text{CO} + \text{CO}_2$ atmospheres in the temperature range 1573 to 1773K, β -cristobalite is more likely to form. For comparison, the results of this study have been extrapolated using Janaf data /15/ on β -quartz to β -cristobalite transformation. The results are in reasonable agreement with the data of Campbell and Roeder /4/, especially in view of the uncertainties in thermodynamic data on different modifications of silica. Earlier free energy measurements /3-6/ cannot be fully relied upon for evaluation of thermodynamic data, in view of the ambiguity in the crystal state of SiO_2 .

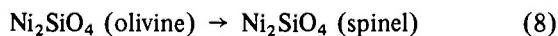
A more rigorous comparison is provided by the calorimetric measurements of Navrotsky /7/, who reports $\Delta H_{965}^\circ = (-13.9) \pm 1.9$ kJ for reaction (4). This is in excellent agreement with the "second law" enthalpy change of $(-13.05) \pm 1.5$ kJ obtained in this study with β -quartz as the reference material for silica. Careful heat capacity measurements from low temperatures up to 1600K can provide further refinement of data on Ni_2SiO_4 (olivine).

The results of this study, as plotted in Fig. 5, do not support the decomposition of Ni_2SiO_4 to NiO and SiO_2 (β -cristobalite) shown on the phase diagram of Phillips *et al.* /2/. The discrepancy may be partly due to Janaf data /15/ on β -cristobalite. However, a hot stage microscopic examination of Ni_2SiO_4 under argon indicated incongruent melting to NiO and a silicate melt at 1868 (± 20) K, in agreement with high pressure melting behaviour reported by Ma /16/. Phase relations in the NiO- SiO_2 system at temperatures above 1700K therefore require redetermination with

careful attention to various crystallographic forms of silica.

4.2. Gibbs' Energy of Formation of Ni_2SiO_4 (spinel)

Ma /16/ and Akimoto *et al.* /17/ have demonstrated the reversibility of high pressure olivine to spinel transition in Ni_2SiO_4 in the temperature range 900 to 1500K. Based on $\Delta V^\circ = -3.39 \text{ cm}^3$ /18, 19/, independent of pressure for this transition, the following equations are obtained for the Gibbs' energy change for the transition,



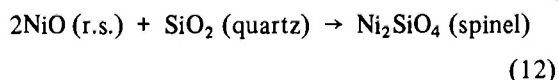
$$\Delta G^\circ = (5,330 + 4.07 T) \text{ J mol}^{-1} \quad /17/ \quad (9)$$

$$= (6,820 + 4.0 T) \text{ J mol}^{-1} \quad /16/ \quad (10)$$

Navrotsky /20/ has measured the enthalpy change for the transition as $(5,980) \pm 2900 \text{ J mol}^{-1}$ by oxide melt solution calorimetry at 986K. The calorimetric result lies between the two "second law" values obtained from the variation of the transition pressure with temperature. Based on the three studies, the Gibbs' energy change for reaction (8) is evaluated as,

$$\Delta G^\circ = (6,080 + 4.03 T) \pm 700 \text{ J mol}^{-1} \quad (11)$$

Combining this with the Gibbs' energy of formation of the olivine obtained in this study, one obtains for the formation of the spinel from component oxides,



$$\Delta G^\circ = (-6,970 + 9.70 T) \pm 710 \text{ J mol}^{-1} \quad (13)$$

4.3. Conduction Mechanism in CaF_2 with Oxygen Electrodes

The results reported in section 3.2 clearly indicate that the emf of the cell is controlled by the activity of CaO at the electrode/electrolyte interface, in addition to the difference in oxygen potential between the two electrodes. This suggests that CaO is involved in the process of emf generation in solid state cells with CaF_2 electrolyte and oxygen (oxide) electrodes. If oxygen ions were mobile in CaF_2 with a transport number $t_{\text{O}^{2-}} \approx 0.3$, as suggested by Chou and Rapp /9/, the cell would not have developed the large negative potentials. Since fluorine potential at each electrode

is developed through a slow exchange reaction, the cell would have produced a direct response to the oxygen potential gradient, if oxygen ions were mobile. Even if exchange reaction (1) is assumed to be rapid and the thermodynamic capacities $(\partial n_j / \partial \mu_j)$, where n_j and μ_j are the number of moles and chemical potential of species j) of both oxygen and fluorine are approximately equal, the electrochemical cell should respond to that chemical potential gradient (in the present case, oxygen) which results in the lowest numerical value of emf. The experimental results clearly show a final emf response to fluorine chemical potential at the electrodes, and not to oxygen potential. The present results therefore provide strong evidence against mixed anionic conduction in CaF_2 suggested by Chou and Rapp /9/. Further experiments to support the absence of significant oxygen ion transport will be reported in a separate paper. The use of CaF_2 electrolyte for oxygen potential measurements must be restricted to those systems where there is no interaction between the electrode components and CaO in CaF_2 .

5. SUMMARY

Gibbs' energy of formation of Ni_2SiO_4 (olivine) has been firmly established by solid state galvanic cell measurements in the temperature range 925 to 1375K. Doubts regarding the crystal modifications of quartz used in earlier investigations have been clarified. The new results are in agreement with high temperature calorimetric data. The present results support the decomposition of Ni_2SiO_4 (olivine) to NiO and a liquid silicate, and not to NiO and cristobalite as suggested by Phillips *et al.* /2/.

The results of this study on Ni_2SiO_4 (olivine) have been combined with independent high pressure and calorimetric measurements reported in the literature to derive values for the Gibbs' energy of formation of the spinel form of Ni_2SiO_4 .

Results obtained with a galvanic cell using CaF_2 solid electrolyte and oxide electrodes indicate that the emf is affected by the activity of CaO at the electrode/electrolyte interface. This finding argues against the postulate of mixed anionic transport proposed by Chou and Rapp /9/.

REFERENCES

1. RINGWOOD, A.E., *Geochim. Cosmochim. Acta*, **10**: 297 (1956).
 2. PHILLIPS, B., HUTTA, J.J. and WARSHAW, I., *J. Am. Ceram. Soc.*, **40**: 579 (1963).
 3. TAYLOR, R.W. and SCHMALZRIED, H., *J. Phys. Chem.*, **68**: 2444 (1964).
 4. CAMPBELL, F.E. and ROEDER, P., *Am. Mineral.*, **53**: 257 (1968).
 5. LEBEDEV, B.G. and LEVITSKII, V.A., *Russ. J. Phys. Chem.*, **35**: 1380 (1961).
 6. RÖG, G. and KOZHUWSKA-RÖG, A., *Electrochim. Acta*, **30**: 335 (1985).
 7. NAVROTSKY, A., *J. Inorg. Nucl. Chem.*, **33**: 4035 (1971).
 8. NOTIN, M., CUNAT, C. and HERTZ, J., *Thermochim. Acta*, **33**: 175 (1979).
 9. CHOU, S.F. and RAPP, R.A., *J. Electrochem. Soc.*, **130**: 506 (1983).
 10. RAMANARAYANAN, T.A., NARULA, M.L. and WORRELL, W.L., *J. Electrochem. Soc.*, **126**: 1360 (1979).
 11. JACOB, K.T., RAO, D.B. and NELSON, H.G., *J. Electrochem. Soc.*, **125**: 758 (1978).
 12. STEELE, B.C.H., "Electromotive Force Measurements in High Temperature Systems", Ed. C.B. Alcock, Inst. Min. Met., London, p. 3 (1968).
 13. LEVIN, E.M. and McMURDIE, H.F., "Phase Diagrams for Ceramists", Supplements, Am. Ceram. Soc., (1969) and (1975).
 14. BENZ, R. and WAGNER, C., *J. Phys. Chem.*, **65**: 1308 (1961).
 15. STULL, D.R., *et al.*, Janaf Thermochemical Tables, NSRDS-NBS 37, U.S. Department of Commerce, Washington (1970).
 16. MA, C.B., *J. Geophys. Res.*, **79**: 3321 (1974).
 17. AKIMOTO, S., FUJISAWA, H. and KATSURA, T., *J. Geophys. Res.*, **70**: 1969 (1965).
 18. LAGER, G.A. and MEAGHER, E.P., *Am. Mineral.*, **63**: 365 (1978).
 19. YAGI, T., MARUMO, F. and AKIMOTO, S., *Am. Mineral.*, **59**: 486 (1974).
 20. NAVROTSKY, A., *Earth and Planet. Sci. Lett.*, **19**: 471 (1973).
-